



Ionic/Electronic Conducting Characteristics of LiFePO₄ Cathode Materials

The Determining Factors for High Rate Performance

Chunsheng Wang*^z and Jian Hong**

Department of Chemical Engineering and Center for Manufacturing Research,
Tennessee Technological University, Cookeville, Tennessee 38505, USA

The Li⁺ ion diffusion coefficient of lithium iron phosphate (LiFePO₄) cathode materials should not be measured by the standard method because there is no composition variation but the movement of the LiFePO₄/FePO₄ interface during Li insertion/extraction. A method to measure the intrinsic electronic and ionic conductivity of mixed conductive LiFePO₄ was reported, for the first time, based on the conductivity measurements of mixed conductive solid electrolyte using blocking electrodes. The conductivities of the three LiFePO₄ materials (mixed electronic/ionic conductor, electronic conductor, and ionic conductor), were measured using the proposed method, and the electronic and ionic conductivities were linked with their electrochemical reaction kinetics and rate capabilities. These LiFePO₄ samples have the same X-ray diffraction crystal structure and similar particle size, but different rate performance due to the difference in the ionic/electronic conductivity. The rate performance of the mixed electronic/ionic conductive LiFePO₄ is much higher than that of the electronic conductive LiFePO₄ and the ionic conductive LiFePO₄.

© 2007 The Electrochemical Society. [DOI: 10.1149/1.2409768] All rights reserved.

Manuscript submitted May 30, 2006; revised manuscript received October 12, 2006. Available electronically January 3, 2007.

LiFePO₄ demonstrates a substantial reversible capacity at around 3.4 V, low cost, long cycle life due to small volume change (6.8%), and is environmentally benign. However, the pristine compound has the disadvantage of poor rate performance due to its low electronic conductivity ($\sim 10^{-9}$ S cm⁻¹). Several methods have been used to enhance the inherent electronic conductivity, such as carbon coating,¹ super-valence ion doping in the Li-site,^{2,3} and nano-networking of electronic conductive metal-rich phosphides forming at high temperatures.⁴ However, it seems that the corresponding electrochemical performance does not improve as one would expect by electronic conductivity enhancement. For doped LiFePO₄ with high electronic conductivity, the ionic conductivity (or diffusion ability) may become a limiting step, as evidenced by the excellent rate performance of LiFePO₄ nanofibers in carbon matrix⁵ and nanosize (140 nm) pure LiFePO₄ without carbon coating.⁶ Another way to improve the rate performance of LiFePO₄ is to increase Li⁺ ionic mobility and diffusion coefficient by bivalent cation (such as Ni, Co, and Mg) doping.⁷

Although, ionic conductivity is a key factor for achieving high performance from LiFePO₄, it is very difficult to accurately measure the diffusion coefficient of Li-ion in LiFePO₄ by standard methods such as electrochemical impedance spectroscopy (EIS) and galvanostatic intermittent titration (GITT) in three-electrode cell due to a very flat charge-discharge potential induced by the phase transformation between LiFePO₄ and FePO₄.⁸ EIS and GITT using a three-electrode cell for diffusion coefficient measurement were proven to be valid only for solid solution reactions.⁸ Three-electrode-cell EIS and GITT can only measure the “effective” diffusion coefficient of the electrode with two-phase reaction.⁸ The “effective” diffusion coefficients measured using three-electrode cell were 1.8×10^{-14} for LiFePO₄ and 2×10^{-16} cm² s⁻¹ for FePO₄,⁸ which is 7 orders less than the theoretical calculation (10^{-8} cm² s⁻¹ for LiFePO₄ and 10^{-7} for FePO₄).⁹ Moreover, the faster charge (Li extraction) capability relative to the discharge (Li insertion) capability also indicates that the Li diffusion in FePO₄ should be higher than that in LiFePO₄,¹⁰ which is in agreement with the theoretical calculations,⁹ but is in a reverse order of the effective diffusion coefficient values obtained using EIS and GITT.⁸ Therefore, a more accurate method is

needed for measurement of Li ion conductivity (or diffusion coefficient) in the electrode with phase transformation reaction during charge/discharge.

Recently, it has been reported that the electronic and ionic conductivities of a mixed electronic/ionic conductor can be measured by conductive impedance analysis using a blocking electrode (single-electrode). This method has been successfully used to measure the ionic and electronic conductivity of the solid electrolyte for a solid oxide fuel cell.¹¹ Because the diffusion coefficient of the Li-ion can be calculated from the Li-ion conductivity using the Nernst-Einstein equation, this method can be used to determine the Li-ion diffusion coefficient of the mixed conductive electrode. The phase transformation between Li_{0.89}FePO₄ and Li_{0.05}FePO₄ with a very flat potential plateau¹² will not happen during conductive EIS measurement with a small (<5 mV) signal amplitude because there is no Li content change (no Li intercalation reaction) in the ionic blocking electrode, thus no phase transformation occurs. Because there is no material limitation for conductive EIS measurement, this method has been widely used to determine the ionic conductivity of electrolytes. To the authors' best knowledge, there is no known report on using this method to measure the ionic conductivity of cathode electrode of Li-ion battery.

In this work, the intrinsic electronic and ionic conductivity of mixed conductive LiFePO₄ was measured, for the first time, based on the conductivity measurements of mixed conductive solid electrolyte using blocking electrodes. Moreover, the rate performances of three LiFePO₄ samples with different electronic/ionic conducting properties were also compared to investigate the relationship between the ionic/electronic conductivity of LiFePO₄ and rate capability.

Experimental

Material preparation and characterization.—LiFePO₄ materials with different electronic/ionic conductivity were prepared. Pristine (pure) Li⁺ ion conductive LiFePO₄ has a very low electronic conductivity, and can be considered as an ionic conductor and electronic insulator. Therefore, pristine LiFePO₄ prepared from non-carbon-containing precursors (Fe₃(PO₄)₂·8H₂O) + Li₃PO₄) reported by Herle⁴ was used as a control sample (sample C). Carbon-containing precursors and heat treatment under Ar + 5%H₂ were used for preparation of the electronic conductive LiFePO₄ sample. It was reported that Mg and Ni in LiFe_{0.9}M_{0.1}PO₄ [M = Mg, Ni] can weaken the Li-O interaction, thus potentially enhancing the ionic mobility and diffusion coefficient of LiFe_{0.9}M_{0.1}PO₄, where Mg is more effective than Ni.⁷ Therefore, carbon-containing Mg

* Electrochemical Society Active Member.

** Electrochemical Society Student Member.

^z E-mail: cswang@tntech.edu

and Ni were used for Fe-site doping in LiFePO_4 to tune the electronic and ionic conductivity. For $\text{LiFe}_{0.95}\text{Mg}_{0.05}\text{PO}_4$ (sample A), $\text{LiFe}_{0.95}\text{Ni}_{0.05}\text{PO}_4$ (sample B) preparation, lithium carbonate (Aldrich, >99%), iron(II) oxalate tetrahydrate (Aldrich, >99%), ammonium phosphate (Aldrich, >99%), magnesium oxalate (Alfa, >99%) and nickel(II) oxalate (Alfa, >99%) and were used as the precursors. The synthesis followed previously reported directions.² The stoichiometric precursors were ball-milled in acetone for 4 days inside a plastic bottle. Then the raw materials were dried, ground and sieved before fired in an argon (with 5% H_2) environment. The ground precursors were first decomposed at 350°C for 5 h for the $\text{LiFe}_{0.95}\text{Ni}_{0.05}\text{PO}_4$ sample (sample B) and 9.5 h for the $\text{LiFe}_{0.95}\text{Mg}_{0.05}\text{PO}_4$ sample (sample A) to drive away any decomposing gases. A long heat-treatment time at 350°C for $\text{LiFe}_{0.95}\text{Mg}_{0.05}\text{PO}_4$ was used to reduce the remaining carbon content in $\text{LiFe}_{0.95}\text{Mg}_{0.05}\text{PO}_4$, thus decreasing its electronic conductivity. After that, the temperature was directly raised to 700°C for 5 h, and then slowly cooled to room temperature. Therefore, the $\text{LiFe}_{0.95}\text{Ni}_{0.05}\text{PO}_4$ sample prepared using the above method, is expected to have a higher electronic conductivity but lower ionic conductivity than that of $\text{LiFe}_{0.95}\text{Mg}_{0.05}\text{PO}_4$ because (i) Mg can more effectively increase the Li^+ ion mobility by weakening the Li-O bond more than Ni can enhance it,⁷ (ii) an incomplete carbon film coating on $\text{LiFe}_{0.95}\text{Mg}_{0.05}\text{PO}_4$ due to low carbon content might allow lithium to pass without having to tunnel through the carbon film, with only a minor decrease in the ionic conductivity.¹³

The crystalline phases of the LiFePO_4 powders were identified by X-ray diffraction (Rigaku DMAX-B) analysis at room temperature using Cu $\text{K}\alpha$ radiation. The diffraction data were collected at 0.02° step widths over a 2θ range from 10 to 90° .

Electronic and ionic conductivity measurement.—The pellets used for the electronic and ionic conductivity measurement were prepared by die-pressing three $\text{LiFe}_{1-x}\text{M}_x\text{PO}_4$ ($\text{M} = \text{Mg}, \text{Ni}, x = 0, 0.05$) powder samples (without carbon and binders and a pressure of 1.5 ton/cm^2), and then coating them with an Ag conductor paste on both sides to form the blocking electrodes. The size of the pellets was around $0.6\text{--}1.3 \text{ cm}$ diam and $0.05\text{--}0.1 \text{ cm}$ thick. The electronic/ionic conductivities of the three samples at the temperatures of $-30, -10, 25, 40, 60,$ and 80°C were measured using a Solartron PRA 1260 frequency response analyzer with a Solartron model 1287 electrochemical interface and a frequency range from 10^6 Hz to 1.0 mHz at a potentiostatic sine wave signal amplitude of 5 mV . For comparison, the electronic conductivities of three samples were also tested by linear voltage scanning method at a scanning rate of 1 mV/s from 0 to 0.2 V using a Solartron 1287. The electronic conductivities measured by two methods were nearly identical.

Electrochemical performance measurements.—The electrodes used for electrochemical measurement consisted of 78% LiFePO_4 powder, 8.5% carbon black, and 13.5% polyvinylidene fluoride (PVdF, Kynar, Elf-Atochem) in a 1-methyl-2-pyrrolidinone solvent. Then the mixtures were coated onto an Al foil current collector to form a disk electrode with a surface geometric area of 1.5 cm^2 containing ca. 10 mg of active LiFePO_4 . After drying in an oven at 120°C , the disk electrodes were pressed with a pressure of 1 ton/cm^2 for 10 min. The electrochemical reaction kinetics of the modified LiFePO_4 samples was measured in a three-electrode cell of conventional design, with lithium foil as the counter and reference electrodes using a Solartron PRA 1260/1287 and a frequency range from 10^6 Hz to 1.0 mHz at a potentiostatic sine wave signal amplitude of 5 mV . Charge and discharge characteristics of electrodes in three-electrode cells were measured at a room temperature between 2.5 and 4.2 V in a liquid electrolyte composed of 1.0 M LiPF_6 in EC-DEC-DMC-EMC (1:1:1:3 by volume) (Ferro Corporation) using an Arbin Corporation (College Station, TX) automatic battery cyclers.

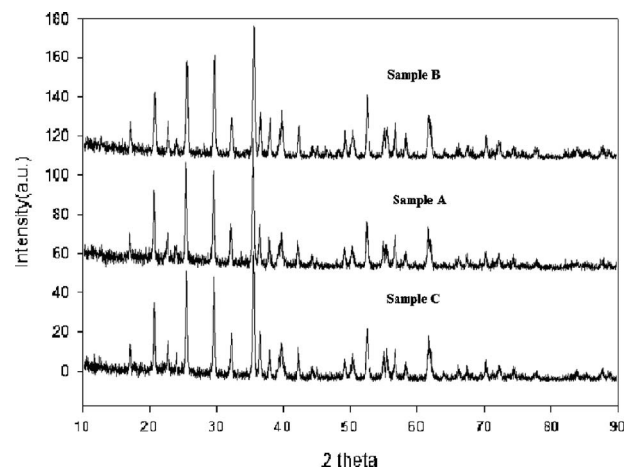


Figure 1. XRD patterns of the mixed conductive ($\text{LiFe}_{0.95}\text{Mg}_{0.05}\text{PO}_4$, sample A), electronic conductive ($\text{LiFe}_{0.95}\text{Ni}_{0.05}\text{PO}_4$, sample B), and ionic conductive (LiFePO_4 , sample C) powders.

Results and Discussion

Structural properties.—The $\text{LiFe}_{0.95}\text{Mg}_{0.05}\text{PO}_4$ sample (sample A), $\text{LiFe}_{0.95}\text{Ni}_{0.05}\text{PO}_4$ sample (sample B), and pure LiFePO_4 sample (sample C) powders were analyzed with XRD to verify phase purity as shown in Fig. 1. Comparison of the powder pattern for all three samples indicates that they are well crystallized in the orthorhombic structure of LiFePO_4 , and there are no detectable impurity phases. Scanning electron microscopy (SEM) images of three LiFePO_4 samples (not shown here) indicates that the three powders consist of a similar aggregate particle with individual particle sizes expected to be much smaller than $1 \mu\text{m}$.

Ionic and electronic conductivity measurements.—Figure 2 shows the typical impedance plots of $\text{LiFe}_{0.95}\text{Mg}_{0.05}\text{PO}_4$ at different temperatures. The depressed semicircle in Fig. 2 suggests that $\text{LiFe}_{0.95}\text{Mg}_{0.05}\text{PO}_4$ is a mixed electronic and ionic conductive material. The electrochemical impedance frequency response of mixed electronic/ionic conductive materials used as an electrolyte has been considered by Jamnik,¹¹ and was used to analyze the impedance of $\text{LiFe}_{0.95}\text{Mg}_{0.05}\text{PO}_4$. The equivalent circuit of mixed conductors developed by Jamnik was further simplified as a parallel combination of electronic resistance and ionic resistance, which is in serial with a capacitor (Fig. 2), and used to fit the impedance data of the $\text{LiFe}_{0.95}\text{Mg}_{0.05}\text{PO}_4$ sample. To fit the depressed semicircles, which is properly induced by the inhomogeneous and distribution (dispersion) of physical property of the electrodes, a constant phase ele-

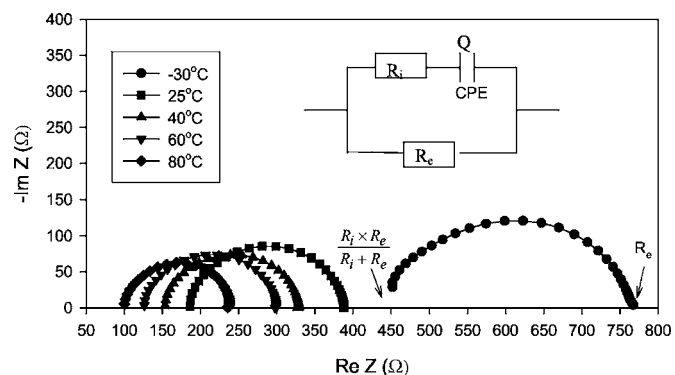


Figure 2. The conductive impedances of $\text{LiFe}_{0.95}\text{Mg}_{0.05}\text{PO}_4$ (sample A) at different temperatures. The inset is the equivalent circuit for mixed conductive materials. The thickness and surface area of disk electrode were 0.064 cm and 1 cm^2 , respectively.

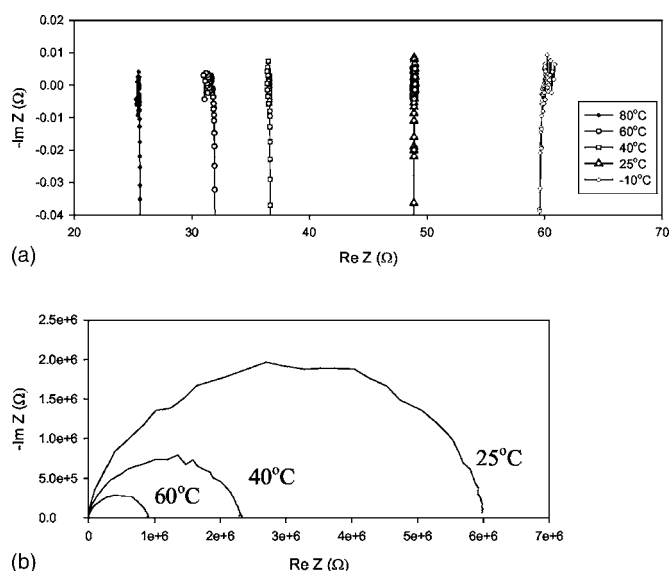


Figure 3. The conductive impedances of $\text{LiFe}_{0.95}\text{Ni}_{0.05}\text{PO}_4$ B (sample) (a) and LiFePO_4 (sample C) (b) at different temperatures.

ment (CPE) was used to replace capacitance in Fig. 4. According to the equivalent circuit inserted in Fig. 2, the intersection of the high-frequency (1 MHz) line with the real axis is the resistance of the electronic and ionic resistance in parallel ($R_e R_i / (R_e + R_i)$), and the intersection of the low-frequency (0.001 Hz) line with the real axis is the electronic resistance (R_e). Unlike the $\text{LiFe}_{0.95}\text{Mg}_{0.05}\text{PO}_4$ sample, the impedance plot of the $\text{LiFe}_{0.95}\text{Ni}_{0.05}\text{PO}_4$ sample is represented by an inductive line with a very small circle (Fig. 3a), indicating almost a pure electronic conductor. The inductive line in the high-frequency range is an instrumental artifact.¹⁴ In contrast, the impedance plot of the third sample (pure LiFePO_4) demonstrates a very large depressed semicircle at different temperatures (Fig. 3b), indicating a very low electronic conductivity (3.7×10^{-9} S/cm) but a reasonable ionic conductivity (5×10^{-5} S/cm). Actually, sample C can be considered as an ionic conductor and electronic insulator due to its low electronic conductivity. The electronic and ionic conductivities of these three samples at different temperatures were calculated based on the equivalent circuit inserted in Fig. 2 and are summarized in Table I. $\text{LiFe}_{0.95}\text{Mg}_{0.05}\text{PO}_4$ is a mixed electronic/ionic conductor because of the comparable electronic and ionic conductivity. $\text{LiFe}_{0.95}\text{Ni}_{0.05}\text{PO}_4$ is an electronic conductor while pure LiFePO_4 is an ionic conductor. The electronic conductivity at room temperature decreases in the following trend: $\text{LiFe}_{0.95}\text{Ni}_{0.05}\text{PO}_4 > \text{LiFe}_{0.95}\text{Mg}_{0.05}\text{PO}_4 > \text{LiFePO}_4$, while the ionic conductivity decreases in an order of $\text{LiFe}_{0.95}\text{Mg}_{0.05}\text{PO}_4 > \text{LiFe}_{0.95}\text{Ni}_{0.05}\text{PO}_4 = \text{LiFePO}_4$. The electronic conductivity variation may be attributed mainly to the carbon content difference in the three samples because of (i) carbon-containing precursors for $\text{LiFe}_{0.95}\text{Mg}_{0.05}\text{PO}_4$ and

$\text{LiFe}_{0.95}\text{Ni}_{0.05}\text{PO}_4$ during synthesis, and noncarbon precursors for LiFePO_4 , (ii) longer heat-treatment time at 350°C for $\text{LiFe}_{0.95}\text{Mg}_{0.05}\text{PO}_4$ than that of $\text{LiFe}_{0.95}\text{Ni}_{0.05}\text{PO}_4$, which blows away more carbon by $\text{Ar} + \text{H}_2$. Ni doping in LiFePO_4 did not change the ionic conductivity, but Mg does. The reasons for three times higher ionic conductivity of $\text{LiFe}_{0.95}\text{Mg}_{0.05}\text{PO}_4$ as compared to $\text{LiFe}_{0.95}\text{Ni}_{0.05}\text{PO}_4$ and LiFePO_4 are not clear at the present time. It is probably attributed to a combination of effects such as a significant weakening of the Li-O bonding by Mg,⁷ and a low carbon coating in $\text{LiFe}_{0.95}\text{Mg}_{0.05}\text{PO}_4$. Recently, the structural characterization and electrochemical performance of $\text{LiFe}_{0.9}\text{Mg}_{0.1}\text{PO}_4$ has been investigated by several researchers.^{7,15,16} The Fe substitution by Mg was confirmed by the shrinkage of the cell volume due to the shrinkage in a and c lattice parameter values.^{7,15} X-ray photoelectron spectroscopy (XPS) analysis on the chemical environment variation of Li and O in LiFePO_4 after 10% Mg doping indicated that the binding energy of O 1s and Li 1s shift down 0.5 and 0.2 eV, respectively.⁷ DFT simulation shows that the Li-O bond length in LiFePO_4 increased from 2.05 Å for LiFePO_4 to 2.06 Å for $\text{LiFe}_{0.9}\text{Mg}_{0.1}\text{PO}_4$. Both results indicated that Li-O interaction is weakened by Mg doping.⁷ It may also be possible that the improvement in ionic conductivity of $\text{LiFe}_{0.95}\text{Mg}_{0.05}\text{PO}_4$ was attributed to the differences in the microstructure and carbon distribution rather than doping effects. Because LiNiPO_4 has the same structure as LiFePO_4 , Fe in LiFePO_4 can be easily replaced by Ni as confirmed by the researchers.¹⁷⁻¹⁹ The exact mechanism for the high ionic conductivity of $\text{LiFe}_{0.95}\text{Mg}_{0.05}\text{PO}_4$ is not clear yet and will be the subject for future research. The objective of this paper is not to understand the mechanism but rather to report a method to measure the intrinsic electronic and ionic conductivity of mixed conductive LiFePO_4 , and the effect of electronic/ionic conductivity on the rate performance of the LiFePO_4 cathode.

Rate capacity.— Figure 4 illustrates the discharge performance of the three samples at different discharge currents. The discharge capacity of pure LiFePO_4 quickly decreases with increasing discharge current because of the low electronic conductivity (3.79×10^{-9} S/cm). For the same reason, the discharge voltage plateau of LiFePO_4 is much lower than the equilibrium voltage (3.4 V) of LiFePO_4 , even at a low discharge current (0.1 C). As expected, the rate performance of the electronic conductive $\text{LiFe}_{0.95}\text{Ni}_{0.05}\text{PO}_4$ is much better than that of pure LiFePO_4 , indicating that increasing the electronic conductivity of pristine LiFePO_4 significantly improved the rate performance, which is in agreement with reported results.⁷ Surprisingly, $\text{LiFe}_{0.95}\text{Mg}_{0.05}\text{PO}_4$, with a balanced electronic and ionic conductivity, has the best rate performance even though its electronic conductivity (1.65×10^{-4} S/cm) is lower than $\text{LiFe}_{0.95}\text{Ni}_{0.05}\text{PO}_4$ (6.40×10^{-3} S/cm). Similar results have also been reported by Chen's group.^{7,20} One possible reason for the high rate capability of $\text{LiFe}_{0.95}\text{Mg}_{0.05}\text{PO}_4$ is attributed to a balanced electronic and ionic conductivity.

The possible mechanism for the high rate performance of ionic/electronic balanced LiFePO_4 can be explained as follows. LiFePO_4

Table I. The electronic and ionic conductivity of three LiFePO_4 samples.

Temperature (°C)	Sample A $\text{LiFe}_{0.95}\text{Mg}_{0.05}\text{PO}_4$		Sample B $\text{LiFe}_{0.95}\text{Ni}_{0.05}\text{PO}_4$		Sample C LiFePO_4	
	σ_e (S/cm)	σ_i (S/cm)	σ_e (S/cm)	σ_i (S/cm)	σ_e (S/cm)	σ_i (S/cm)
-30	8.31×10^{-5}	5.91×10^{-5}	3.90×10^{-3}	—	—	—
-10	—	—	4.68×10^{-3}	—	—	—
25	1.65×10^{-4}	1.79×10^{-4}	6.40×10^{-3}	5.04×10^{-5}	3.7×10^{-9}	5.0×10^{-5}
40	1.91×10^{-4}	2.22×10^{-4}	8.30×10^{-3}	—	7.40×10^{-9}	7.80×10^{-5}
60	2.21×10^{-4}	2.83×10^{-4}	9.00×10^{-3}	—	2.04×10^{-8}	1.06×10^{-4}
80	2.64×10^{-4}	3.76×10^{-4}	0.01	—	3.50×10^{-8}	1.30×10^{-4}

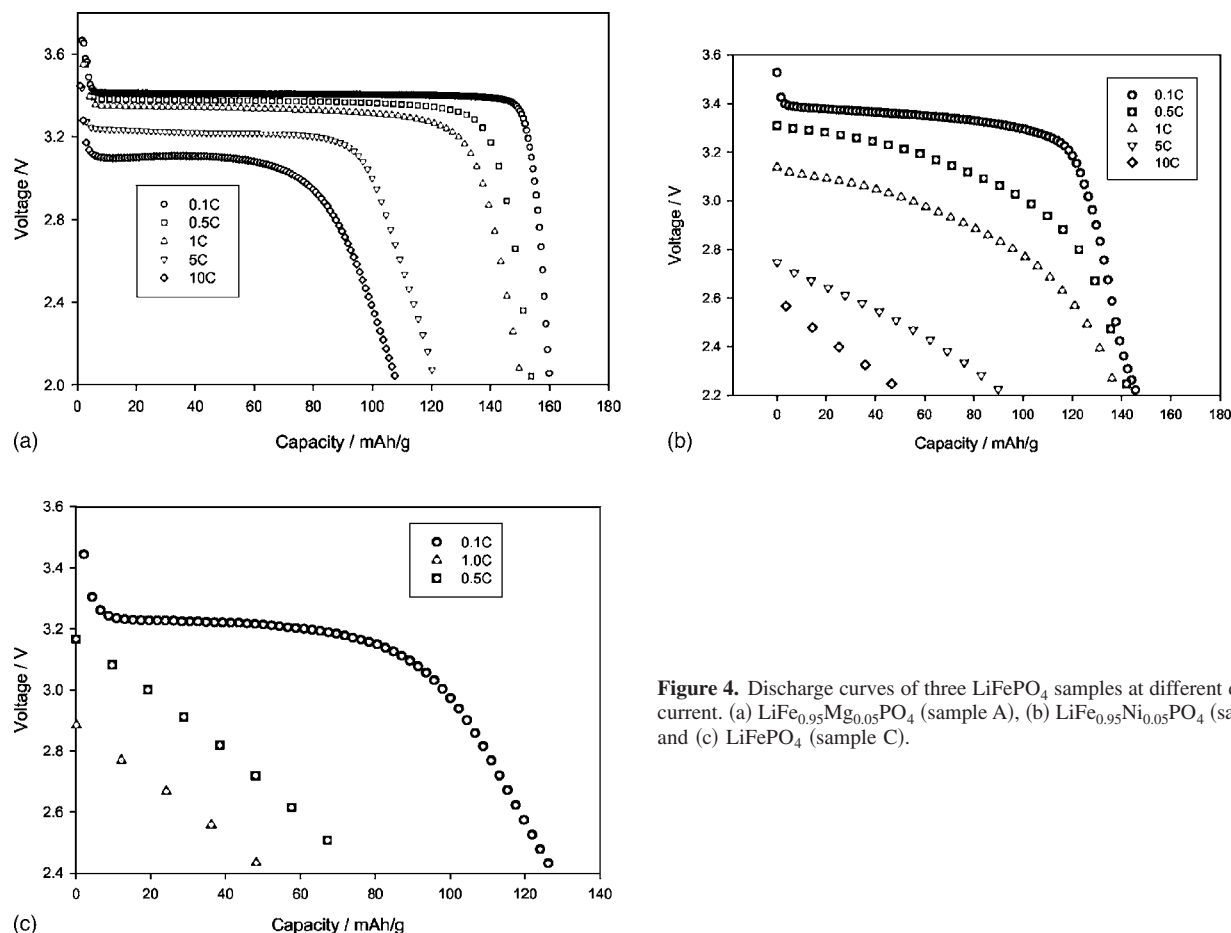


Figure 4. Discharge curves of three LiFePO_4 samples at different discharge current. (a) $\text{LiFe}_{0.95}\text{Mg}_{0.05}\text{PO}_4$ (sample A), (b) $\text{LiFe}_{0.95}\text{Ni}_{0.05}\text{PO}_4$ (sample B), and (c) LiFePO_4 (sample C).

acts as a mixed electronic/ionic conductor. All transport processes of ions and electrons in mixed conductive LiFePO_4 electrodes are caused by gradients in the chemical composition. The Li^+ ion diffusion is always associated with electron transport phenomena, and the internal electrical field generated by the electrons drastically enhances its migration. For LiFePO_4 , the lithium ionic and the electronics can be considered to form a dilute binary electrolyte.²¹ Therefore, the effective diffusion coefficient due to the diffusion and migration can be written as²¹

$$\tilde{D} = \frac{2D_e D_i}{D_e + D_i} \quad [1]$$

where D_i and D_e are the ionic and electronic diffusion coefficients, respectively. A similar equation for the effective diffusion coefficient is given by Riess²²

$$\tilde{D} = k \frac{\sigma_i \times \sigma_e}{\sigma_i + \sigma_e} \quad [2]$$

where σ_i and σ_e are the ionic and electronic conductivities, respectively. These two equations can be converted using the Nernst-Einstein relationship. Both equations suggest that the effective diffusion coefficient (total conductivity of a mixed conductor) is proportional to the electronic and ionic conductivity in parallel, i.e., the total diffusion resistance is equal to the sum of the electronic and ionic resistances. Based on the solid state ionic theory, Jamnik and Maier posited that the overpotential due to the transportation of Li^+ ions and electronics in mixed conductive materials is inversely proportional to the sum of ionic resistance and electronic resistance.²³ If the ionic or electronic conductivity is low in a mixed conductor, ambipolar diffusion will be very sluggish. For pure electronic or ionic conductor materials, the transport rates are de-

termined by the self-diffusion coefficient (not the chemical diffusion coefficient) of the mobile charge carrier solely by the distance over which the charge separation takes place (usually equal or less than the Debye length).²³ For LiFePO_4 , the electronic conductivity (3.7×10^{-9} S/cm) is much lower than its ionic conductivity (5.0×10^{-5} S/cm), indicating that the poor rate performance of LiFePO_4 is mainly attributed to its low electronic conductivity. Although $\text{LiFe}_{0.95}\text{Ni}_{0.05}\text{PO}_4$ has a high electronic conductivity (6.40×10^{-3} S/cm), its low ionic conductivity (5×10^{-6} S/cm) limits its rate capability. The excellent rate performance of the $\text{LiFe}_{0.95}\text{Mg}_{0.05}\text{PO}_4$ is attributable to its balanced electronic and ionic conductivity. For the real electrode mixed with carbon, the ionic conductivity of LiFePO_4 may play a much more important role in its rate capability.²⁴

Electrochemical reaction kinetics measurements.— The Li^+ and electronic transportation (chemical relaxation in particles) impedance can be obtained in a low-frequency region of three-electrode cell EIS. If the concentration polarization, due to the transportation of Li^+ ions and electronics, is inversely proportional to the sum of ionic resistance and electronic resistance,²³ the low-frequency impedance in EIS will be changed accordingly with the sum of the electronic and ionic resistances of LiFePO_4 . Because the particle sizes of all three samples are similar, the electronic and ionic resistivities (reverse of conductivities) of the samples can be used to compare their resistances. Figure 5a shows the reaction impedance of $\text{LiFe}_{0.95}\text{Mg}_{0.05}\text{PO}_4$ at different Li levels and Fig. 5b shows the impedances of $\text{LiFe}_{0.95}\text{Mg}_{0.05}\text{PO}_4$, $\text{LiFe}_{0.95}\text{Ni}_{0.05}\text{PO}_4$ and LiFePO_4 at 50% state of discharge (SOD). The impedances of these three samples show a depressed semicircle in the high-frequency region and a sloping line of variable gradient in the low-frequency region.

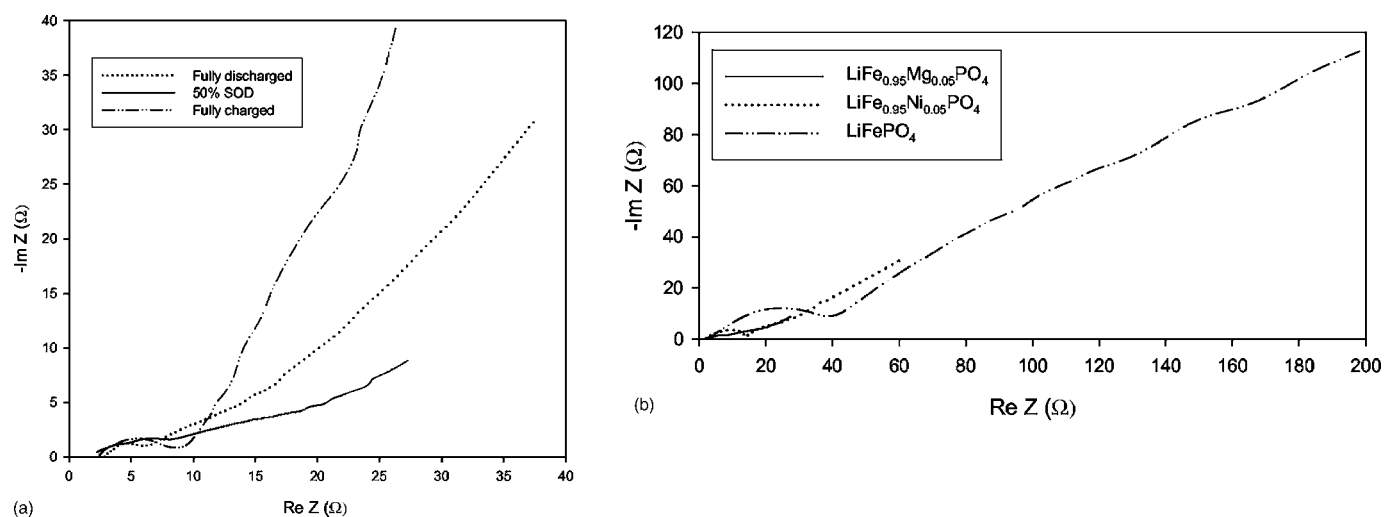


Figure 5. (a) Reaction kinetic impedances of $\text{LiFe}_{0.95}\text{Mg}_{0.05}\text{PO}_4$ at different Li levels and (b) reaction kinetics impedances of $\text{LiFe}_{0.95}\text{Mg}_{0.05}\text{PO}_4$, $\text{LiFe}_{0.95}\text{Ni}_{0.05}\text{PO}_4$ and LiFePO_4 at 50% SOD. EIS were obtained at room temperature after 1 h of relaxation time at each Li contents.

The depressed semicircle, which is dependent of Li levels (Fig. 5a), represents the charge transfer impedance. The sloping line in the low-frequency region is attributed to the sum of the electronic and ionic transporting resistance. The length of the sloping line in the low-frequency region can be used to compare the electronic and ionic transportation resistance. Interestingly, the electronic and ionic transportation resistances at a 50% SOD were much smaller than that at the fully charged and fully discharged state for all three samples (Fig. 5a). The low transportation resistance at 50% SOD can be well explained by the short diffusion length in the 50% SOD using the shrinking-core model.²⁵ At 50% SOD, both the charge transfer resistances (sizes of the semicircle) and low-frequency-transportation resistances of the three samples increased in order of $\text{LiFe}_{0.95}\text{Mg}_{0.05}\text{PO}_4 < \text{LiFe}_{0.95}\text{Ni}_{0.05}\text{PO}_4 < \text{LiFePO}_4$ (Fig. 5b), which is in reverse order of the rate capability (Fig. 4). However, the difference in low-frequency transportation resistances between three samples were much larger than that in charge transfer resistances, which indicated that the differences in the rate performance between the three samples are mainly due to the large changes in the transportation resistance. Because the ionic conductivity of the $\text{LiFe}_{0.95}\text{Ni}_{0.05}\text{PO}_4$ is the same as that of LiFePO_4 , the low transportation resistance of the $\text{LiFe}_{0.95}\text{Ni}_{0.05}\text{PO}_4$ is due to its high electronic conductivity. However, the lower transportation resistance of the $\text{LiFe}_{0.95}\text{Mg}_{0.05}\text{PO}_4$ is due to its higher ionic conductivity. Therefore, the ionic conductivity of the $\text{LiFe}_{0.95}\text{Mg}_{0.05}\text{PO}_4$ plays a more important role than the electronic conductivity, which can be attributed to the carbon black addition into the $\text{LiFe}_{0.95}\text{Mg}_{0.05}\text{PO}_4$ electrode during its rate capability measurement. The electronic conductive carbon black addition increased the electronic conductivity of the electrodes, which lowered the requirement for the electronic conductivity of the electrode materials.

Conclusions

Three $\text{LiFe}_{1-x}\text{M}_x\text{PO}_4$ materials ($\text{M} = \text{Mg}, \text{Ni}, x = 0, 0.05$), classified as an ionic conductor, mixed ionic/electronic conductor, and electronic conductor, respectively, were prepared. The ionic conductivities of these three samples were measured for the first time using EIS and blocking electrodes. As expected, the electronic conductor, $\text{LiFe}_{0.95}\text{Ni}_{0.05}\text{PO}_4$, has a better rate performance than the electronic insulator, LiFePO_4 . Surprisingly, electronic/ionic conductivity balanced $\text{LiFe}_{0.95}\text{Mg}_{0.05}\text{PO}_4$, shows the best rate performance even though its electronic conductivity is lower than electronic conducting $\text{LiFe}_{0.95}\text{Ni}_{0.05}\text{PO}_4$. The excellent reaction kinetics of the mixed

conductor $\text{LiFe}_{0.95}\text{Mg}_{0.05}\text{PO}_4$ is attributed to the very lower transportation resistance as evidenced by the EIS results. This result can be explained by the solid ion transportation theory, which states that the transportation polarization in mixed conductive materials is inversely proportional to the sum of the ionic and electronic resistance.

Tennessee Technological University assisted in meeting the publication costs of this article.

References

1. N. Ravet, J. B. Goodenough, S. Besner, M. Simouneau, P. Hovington, and M. Armand, Abstract, 127, The Electrochemical Society and The Electrochemical Society of Japan Meeting Abstracts, Vol. 99-22, Honolulu, HI, Oct 17-22, 1999.
2. S. Y. Chung, J. Bloking, and Y. Ching, *Nat. Mater.*, **1**, 123 (2002).
3. S. Y. Chung and Y. M. Chiang, *Electrochem. Solid-State Lett.*, **6**, A278 (2003).
4. P. S. Herle, B. Ellis, N. Coombs, and L. F. Nazar, *Nat. Mater.*, **3**, 147 (2004).
5. C. R. Sides, F. Croce, V. Y. Young, C. R. Martin, and B. Scrosati, *Electrochem. Solid-State Lett.*, **8**, A484 (2005).
6. C. Delacourt, P. Poizot, S. Levasseur, and C. Masquelier, *Electrochem. Solid-State Lett.*, **9**, A352 (2006).
7. D. Wang, H. Li, S. Shi, X. Huang, and L. Chen, *Electrochim. Acta*, **50**, 2955 (2005).
8. P. P. Prossini, M. Lisi, D. Zane, and M. Pasquali, *Solid State Ionics*, **148**, 45 (2002).
9. D. Morgan, A. V. Ven, and G. Ceder, *Electrochem. Solid-State Lett.*, **7**, A30 (2004).
10. V. Srinivasan and J. Newman, *Electrochem. Solid-State Lett.*, **9**, A110 (2006).
11. J. Jamnik, *Solid State Ionics*, **157**, 19 (2003).
12. A. Yamada, H. Koizumi, S. Nishimura, N. Sonoyama, R. Kanno, M. Yonemura, T. Nakamura, and Y. Kobayashi, *Nat. Mater.*, **5**, 356 (2006).
13. A. A. Salah, A. Mauger, K. Zaghib, J. B. Goodenough, N. Ravet, M. Gauthier, F. Gendron, and C. M. Julien, *J. Electrochem. Soc.*, **153**, A1692 (2006).
14. C. Wang, I. Kakwan, A. J. Appleby, and F. E. Little, *J. Electroanal. Chem.*, **489**, 55 (2000).
15. J. Barker, M. Y. Saidi, and J. L. Swoyer, *Electrochem. Solid-State Lett.*, **6**, A53 (2003).
16. G. X. Wang, S. Bewlay, J. Yao, J. H. Ahn, S. X. Dou, and H. K. Liu, *Electrochem. Solid-State Lett.*, **7**, A503 (2004).
17. C. V. Ramana, A. Ait-Salah, S. Utsunomiya, U. Becker, A. Mauger, F. Gendron, and C. M. Julien, *Chem. Mater.*, **18**, 3788 (2006).
18. J. S. Yang and J. J. Xu, *J. Electrochem. Soc.*, **153**, A716 (2006).
19. W. Paraguassu, P. T. C. Freire, V. Lemos, S. M. Lala, L. A. Montoro, and J. M. Rosolen, *J. Raman Spectrosc.*, **36**, 213 (2005).
20. C. Ouyang, S. Shi, Z. Wang, X. Huang, and L. Chen, *Phys. Rev. B*, **69**, 104303 (2004).
21. K. Striebel, J. Shim, V. Srinivasan, and J. Newman, *J. Electrochem. Soc.*, **152**, A664 (2005).
22. I. Reiss, *Solid State Ionics*, **157**, 1 (2003).
23. J. Jamnik and J. Maier, *Phys. Chem. Chem. Phys.*, **5**, 5215 (2003).
24. J. M. Tarascon, C. Delacourt, A. S. Prakash, M. Morcrette, M. S. Hegde, and C. Wurm, *Dalton Trans.*, **2004**, 2988.
25. V. Srinivasan and J. Newman, *J. Electrochem. Soc.*, **151**, A1517 (2004).